Heliyon 10 (2024) e33270

Contents lists available at ScienceDirect

Heliyon

journal homepage: www.cell.com/heliyon

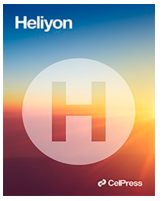

Research article

Development of Versatile, thermally stable, flexible, UV-resistant and antibacterial polyvinyl alcohol-Nanodiamonds composite for efficient food packaging

Saman Iqbal [a,*], Muhammad Shahid Rafique [b], Nida Iqbal [c], Shazia Bashir [d], M. B. Malarvili [e,**], Aftab Ahmad Anjum [f]

[a] Department of Physics, University of the Punjab, Lahore, Pakistan
[b] Department of Physics, University of Engineering and Technology, Lahore, Pakistan
[c] Biomedical Engineering Centre, University of Engineering and Technology, Lahore, Kala Shah Kaku (K.S.K.) Campus, Pakistan
[d] Department of Physics, Government College University, Lahore, Pakistan
[e] Department of Biomedical and Health Science Engineering, Faculty of Electrical Engineering, Universiti Teknologi Malaysia, Skudai, Johor Darul Takzim, Malaysia
[f] Institute of Microbiology, University of Veterinary and Animal Sciences, Lahore, Pakistan

A R T I C L E I N F O

Keywords:
Biodegradable polymer
Nanocomposite
Nanodiamond
Thermal decomposition temperature
Mechanical stability
UV resistance
Antimicrobial properties
Broth microdilution method
Minimum inhabitation concentration

A B S T R A C T

This research paper reports an enhancement of thermal, optical, mechanical and antibacterial activities of the Polyvinyl alcohol–Nanodiamonds (PVA-NDs) composite required for the food packaging industry. The synthesis of composites was done by the wet processing method. The large surface area of NDs facilitated the robust interaction between the hydroxyl group and macromolecular chains of PVA to enhance the hydrogen bonding of PVA with NDs rather than PVA molecules. Thus, a reduction in PVA diffraction peak intensity was reported. NDs improved the thermal stability by preventing the out-diffusion of volatile decomposition products of PVA. The results also revealed an enhancement in tensile strength (~60 MPa) and ductility (~180 %). PVA-NDs composite efficiently blocked the UVC (100 %), most of the part of the UVB (~85 % above 300 nm), and UVA (~58 %). Furthermore, enhanced antibacterial activities were reported for PVA-NDs composite against *E. coli* and *S. aureus*. NDs accumulated around the bacterial cells prevented essential cellular functions and led to death. Hence, this composite could be a promising candidate for safe, thermally stable, strong, flexible, transparent, UV- resistant antibacterial food packaging material.

List of Abbreviations

Polyvinyl alcohol	PVA
Nanodiamonds	NDs
Melting temperature	Tm
thermal decomposition temperature	Td
Polyvinyl pyrrolidone	PVP

(*continued on next page*)

* Corresponding author.
** Corresponding author.
E-mail addresses: samaniqbal.physics@pu.edu.pk (S. Iqbal), malarvili@utm.my (M.B. Malarvili).

https://doi.org/10.1016/j.heliyon.2024.e33270
Received 16 October 2023; Received in revised form 15 June 2024; Accepted 18 June 2024
Available online 18 June 2024

(*continued*)

Titanium dioxide	TiO_2
Graphene oxide	GO
Zinc oxide	ZnO
Staphylococcus aureus	*S.aureus*
Escherichia coli	*E-.coli*
Polyethyleneimine	PEI
Tri-tungsten(vi) oxide	WO_3
Silver	Ag
Carboxylated NDs	cND
X-rays Diffractometer	XRD
Thermogravimeter	TGA
Differential Scanning Calorimetry	DSC
Ultimate tensile tester	UTM
Fourier Transform Infrared Spectrophotometer	FTIR
Minimum Inhabitation Concentration	MIC

1. Introduction

Plastic is vital to the food industry, comprising approximately 56 % of the materials used in food packaging. It contributes to preserve food quality and guarantees food safety during its shelf-life. The list of essential properties includes versatility, economy, functionality, ease of handling, lightweightness, and eco-friendliness. Conventionally utilized non-biodegradable petroleum-based polymeric materials must be replaced with biodegradable ones due to serious health issues and environmental pollution during their manufacturing and disposal [1–6]. Plastic food packaging accounts for over 40 % of total plastic waste worldwide, of which 24.9 % are found in landfills. Although the collection of plastic waste is a slow process, it still poses a significant threat to life and environment of ocean. Moreover, microplastics and other additives finally become part of animals or humans through the food chain [2,3,7,8]. Recent research has confirmed the presence of microplastic (~240,000 particles per litre) in water bottles [9]. The demand to replace synthetic plastic with innovative biodegradable polymers that have large mechanical strength, thermally stable, reasonable optical transparency, UV resistant, antibacterial and antioxidant packaging materials is increasing [2,3,7,8,10].

For over a century, polyvinyl alcohol (PVA) has been known as one of the most highly produced synthetic biodegradable polymers [11]. The exceptional properties of PVA include non-toxicity, high transparency, flexibility, biocompatibility, and chemical resistance [10,12–17]. As a packaging material, PVA appears suitable for resolving environmental pollution problems and decreasing ecological waste. However, inherent brittleness, limited thermal stability, poor UV protection, and ineffectiveness against bacteria impose hurdles in its utilization [13,18,19].

PVA-nanocomposite is an excellent way to enhance traditional polymer properties without influencing their processability [20]. Recent studies have revealed the increasing demand for environmentally friendly, largely available and cost-effective nanofillers. Nanodiamonds (NDs) are a physical modifier in polymer science [21]. The rich surface chemistry of NDs combined with superior thermal, mechanical, optical, and electrical properties provide an excellent opportunity to design the NDs-matrix interface rationally [22,23]. The air-oxidized NDs produce the most stable and uniform aqueous dispersion of PVA-NDs composite [24].

An important parameter to measure the product performance is thermal stability. Polymer thermal stability needs a low melting temperature (Tm) compared to the thermal decomposition temperature (Td). However, PVA possesses Tm (~230 °C) approximately equal to Td (~240 °C) due to high intermolecular and intramolecular hydrogen bonds [19,25,26]. Nanofillers such as Polyvinyl pyrrolidone (PVP)/polyphenols [19], starch fibre [25], artificial marble [26], Soy protein/TiO_2 (Titanium dioxide) [4], etc., play a key role in increasing the thermal resistance of PVA. However, most cases resulted in an unwanted effect on physicochemical characteristics of PVA because of difficult and complex processing. Therefore, thermal stability with optimized mechanical properties has remained a big challenge.

Different researchers tried to enhance both [4,26]. The PVA-NDs composite scaffolds were loaded at different concentrations of NDs using the electrospinning method. The increasing concentration of NDs decreased the crystallinity and boosted the tensile strength and modulus [27]. The results indicated improved thermal, mechanical, and anti-wear properties of PVA-NDs-boric acid [15]. The 3D-printed PVA-NDs composite experienced an enhancement of 200 % indentation modulus [28]. The PVA-NDs composite prepared from the solution casting method reported higher Young's modulus and tensile strength than pristine PVA [24].

Flexibility and tensile strength are important parameters in packaging. In most cases, an increased tensile strength decreased the elongation at the breaking point [29–31]. However, overall enhancement in mechanical performance in both elastic and plastic regions is rarely observed. Famkar et al. [32] reported enhancement in elongation at the breaking point and tensile strength of PVA by inserting polydopamine-coated graphene oxide (GO). This research looked to obtain the same machinal performance with NDs incorporation.

Natural and artificial UV lights induce photo-oxidation and photo-degradation in food products. The masking of UV radiation preserves food components, especially vitamins. As a packaging material, PVA has poor UV resistance [13,33]. Different fillers such as Zinc oxide (ZnO)/plant polyphenols/cellulose [10], Tannic acid [12], TiO_2, waste hump [31], citrate-based fluorophores [33], polyethyleneimine (PEI)- lignin contained cellulose nanofibers [18] were introduced to enhance UV barrier of PVA. Since NDs are effective antioxidants and photostable UV filters, they can be introduced with TiO_2 and ZnO in sunscreen. Anti-UV properties were

preserved even after long simulated solar radiation exposure [34].

Antibacterial packaging materials efficiently suppress bacterial growth, reduce food contamination, and enhance shelf life. Existing research indicates the incorporation of different nanostructures such as GO, tri-tungsten (vi) oxide complex (WO_3), nanorods, silver (Ag), nanoparticles, and ZnO for improvement in antibacterial properties of PVA [17,35,36] [37]. There has been significant interest in NDs as antibacterial material [23,38,39]. Carboxylated NDs (cND) demonstrated excellent antibacterial activity against *E. coli*. Wehling et al. [40] studied NDs with six different oxygen-containing surface groups. The partially oxidized and negatively charged surface of NDs and the anhydride group were responsible for good antibacterial activity against *E. coli* and *B. subtilis*. Similarly, cationic polymer or methanol-modified NDs significantly suppressed *S. aureus* and *E. coli* growth [38]. Beranova et al. [41] correlated the significant reduction of bacterial growth with NDs concentration. Low concentrations (5 μg/mL) were responsible for partial growth inhabitation. In contrast, large concentrations (50 μg/mL) resulted in total growth inhibition.

This research attempted to improve the thermal, optical, mechanical (elastic and plastic region) and antibacterial activities of the PVA matrix by incorporating NDs as nanofillers.

2. Materials and methods

2.1. Materials

PVA was purchased from Sigma-Aldrich. NDs were fabricated from an atmospheric pressure plasma system. The details were mentioned in supporting information.

2.2. Synthesis of PVA-NDs composite

PVA-NDs composites were fabricated using a wet processing (solution casting) method. A stepwise process is explained in Fig. 1.

The concentrations of PVA and NDs are mentioned in Table 1. A colloidal solution was prepared by mixing NDs in DI (deionized) water. For the PVA-NDs composite, 4 g of PVA (Fig. 1(a)) were dissolved into 100 ml of NDs colloidal solution (Fig. 1(b)). It was placed on a magnetic stirrer under constant mechanical stirring. During this process, the temperature remained constant at 80 °C (Fig. 1(c)). After 1 h, a clear and viscous solution was obtained and poured into the Petri dish for casting. An aluminium sheet was already placed inside the Petri dish to remove the film easily. The homogeneous mixture was dried at 40 °C for 48 h (Fig. 1(d)). The prepared film was easily peeled off using a speculum (Fig. 1(e)). An electronic digital micrometer was used to measure film thickness (~200 μm). The final product was available for different properties evaluation (Fig. 1(f)).

The PVA thin film was fabricated by using the same procedure as described above. However, this time PVA (4 gm) was dissolved in DI water (100 ml).

2.3. Characterization of PVA-NDs composite

Structural analysis was done by using X-ray diffractometer (PANAlytical X'Pert PRO Diffractometer with Cu-Kα radiation source). The optical properties were examined with UV–visible spectroscopy (UVD-3200). Fourier Transform Infrared Spectrophotometer (FT/IR-4100 type-A, Jasco) was used to identify functional groups. Thermal decomposition temperature was evaluated with a thermogravimeter (TGA 50 Shimadzu, Japan). A sample was heated to 450 °C in a nitrogen environment (25 mL/min) at 10 °C/min. Thermal behaviour was recorded using differential scanning calorimetry (DSC 60A Shimadzu, Japan) in a nitrogen environment (30 mL/min) at 10 °C/min. The tensile test was performed using an ultimate tensile tester (TIRA test 2810 E6) at 10 mm/min (strain rate). An electronic digital micrometer was used to measure sample thickness. Three samples of each composition were used for each test,

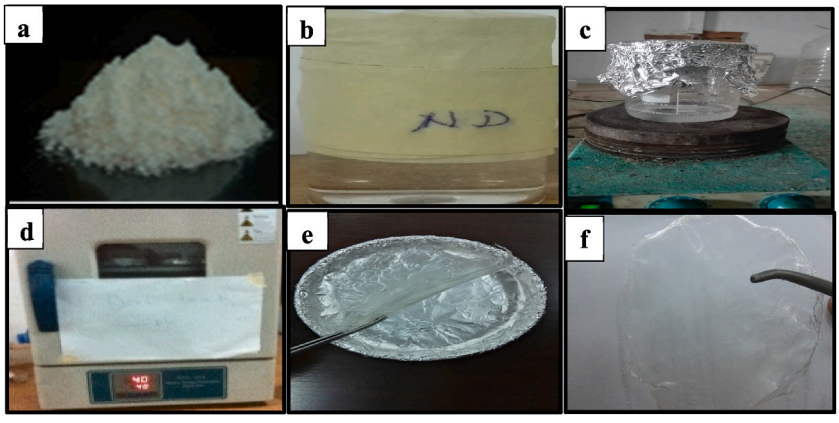

Fig. 1. Complete experimental steps followed for PVA-NDs composites film fabrication (a) PVA, (b) NDs colloidal solution, (c) stirring and heating, (d) drying, (e) peeling off and (f) final product.

Table 1
PVA and NDs concentration.

Sample	PVA (%)	NDs content (mg/ml)
PV	4	0
PND1		0.002
PND2		0.004
PND3		0.008
PND4		0.016

satisfied by ASTM D882-00. For antibacterial testing, *Escherichia Coli, E. coli, (*ATCC No. 25922) and *Staphylococcus Aureus, S. aureus,* (ATCC No. 25923) were procured from University of Veterinary and Animal Sciences, Lahore, Pakistan. The broth microdilution method was selected to find the minimum inhibitory concentration (MIC). The details are discussed earlier [42].

3. Results and discussion

3.1. XRD analysis

XRD patterns for PVA-NDs composites are displayed in Fig. 2. Pure PVA exhibited a strong crystalline reflection at $2\theta = 19^{\circ}$ representing a characteristic peak (101) from a monoclinic unit cell. A broad hump around $2\theta = 40.4^{\circ}$ belongs to (202) reflection of PVA. The semicrystalline nature of PVA is confirmed by strong intermolecular and intramolecular hydrogen bonding between the polymer chains [43–48]. XRD patterns of PVA-NDs composite also show only one major peak ($2\theta = 19^{\circ}$). However, addition of NDs reduced PVA diffraction peak intensity. This is true for all samples(PND1 to PND4). It suggests an enhancement in the amorphous nature of polymer nanocomposite due to the disruption of the PVA crystallinity [24,43–45]. The suppression of PVA crystallinity is related to destroying the order packing of macromolecular chains and making amorphous-type bound layers around the NDs. The steric hindrances induced by NDs decreased the quantity of intact crystalline region within the composite to restrict the crystallization. The large specific surface area of NDs and strong hydrogen bonding led to trapping the PVA molecules onto NDs. As a result, PVA's regular planar zigzag symmetry was destroyed and converted into an amorphous structure on the interfacial region of NDs. Therefore, the overall crystalline structure of PVA decreased [49]. Zhang et al. [46] reported similar results. Low diamond contents in the polymer matrix (PND1, PND2, PND3) did not exhibit any additional peak for a diamond. This suggests that the NDs were fully intercalated without restacking together and homogeneously dispersed into the PVA matrix. However, a very small peak ($2\theta = 41.2^{\circ}$) appeared for sample PND4, at the highest NDs concentration (inset Fig. 2), which might be related to the (100) plane of Lonsdaleite diamond (JCPDS No 19–0268) [22,39,50,51].

Table S1; Table S1 describes the XRD results of the PVA-NDs composite. Scherrer formula was used to calculate the average crystallite size of PV(16.9 nm), PND2 (9.1 nm) and PND4 (9.76 nm) [supporting information]. The increasing concentration of NDs pronounced the decrement in crystallinity. The decrease in the intensity of the crystalline phase (101) accompanied by the increase in the broadness of the peak [supporting information] indicates the change in the ordered packing of the main chain of the polymeric molecules. This signifies the amorphousness in the PVA matrix [43,44,52].

3.2. TGA analysis

The TGA thermograms of both pristine PVA and PVA–NDs composites are presented in Fig. 3(a). Three phases of pristine PVA

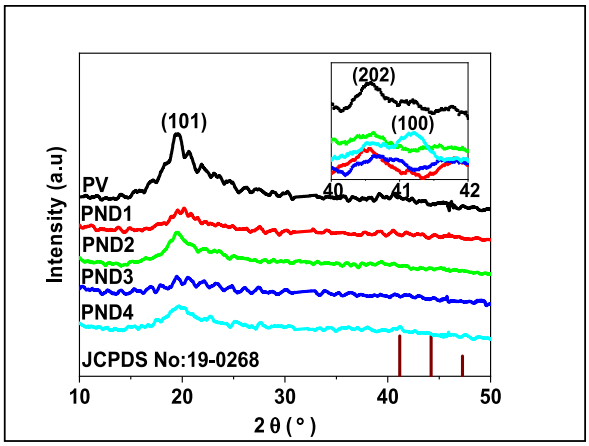

Fig. 2. XRD patterns of PVA-NDs composites. inset is an enlarged image of the diamond peak.

thermal degradation were observed. The first stage (50–150 °C) was related to removal of water molecules, second stage (150–350 °C) was involved in

the thermal degradation of side groups (the loss of hydroxyl group (-OH) in the form of water) and third stage (350–450 °C) was ascribed to main chain scission (cleavage of C–C bond known as carbonization). Significant weight loss of up to 80 % occurred in the last two stages [53,54]. Polymer composites follow the same dehydration and depolymerization process of weight loss but at different temperature ranges. TGA analysis confirmed that the integration of NDs changes the dynamics of PVA. The details of the thermal decomposition temperature and mass loss of the PVA-NDs composites are given in Table S2.

Fig. 3(b) shows the first-order derivatives of TGA curves, representing the temperature at which the maximum mass decrease occurs. The results indicated that the peaks of the first and second decomposition stages became intense and shifted towards higher temperatures after NDs incorporation. A similar trend is observed for all NDs concentrations (PND1 to PND4). Furthermore, the increase in NDs content reduced the high rate of weight loss. Thus, the degradation due to chain stripping or condensation of OH functional groups became slower [22,31]. Meanwhile, the third stage followed the same pattern as the previous stages [43]. The onset temperature of the thermal degradation of the PND4 was 74.26 °C higher than that of pure polymer, PV (Table S2). NDs acted as a barrier, restricting the release of volatile decomposition products in the composites [45]. Hence, a significant enhancement in thermal stability is achieved by the addition of NDs.

Fig. 3(c) shows the relationship between thermal decomposition temperature (Td) with respect to NDs content. An improvement in Td (~320 °C) was observed for PVA-NDs composite (PND1) compared to pristine polymer, PV. This enhancement in thermal stability can be related to the reduced mobility of the PVA chains in the nanocomposite. The chain transfer reactions were restricted, and the degradation process slowed down [55]. However, a small decrease in Td (~305 °C) for PND2 might be related to a slight improvement in crystallinity compared to PND1 (XRD analysis). Further increase in NDs concentration (PND3) increased the Td (~318 °C). Maximum Td (~363 °C) was reported for PND4. Thus, the decomposition takes place at a higher temperature. Heat transfer from an external source encouraged the thermal decomposition of the polymer. However, the accumulation and reassembly of NDs on the surface of the polymer acted as a mass transport barrier for the escape of volatile products during decomposition [56].

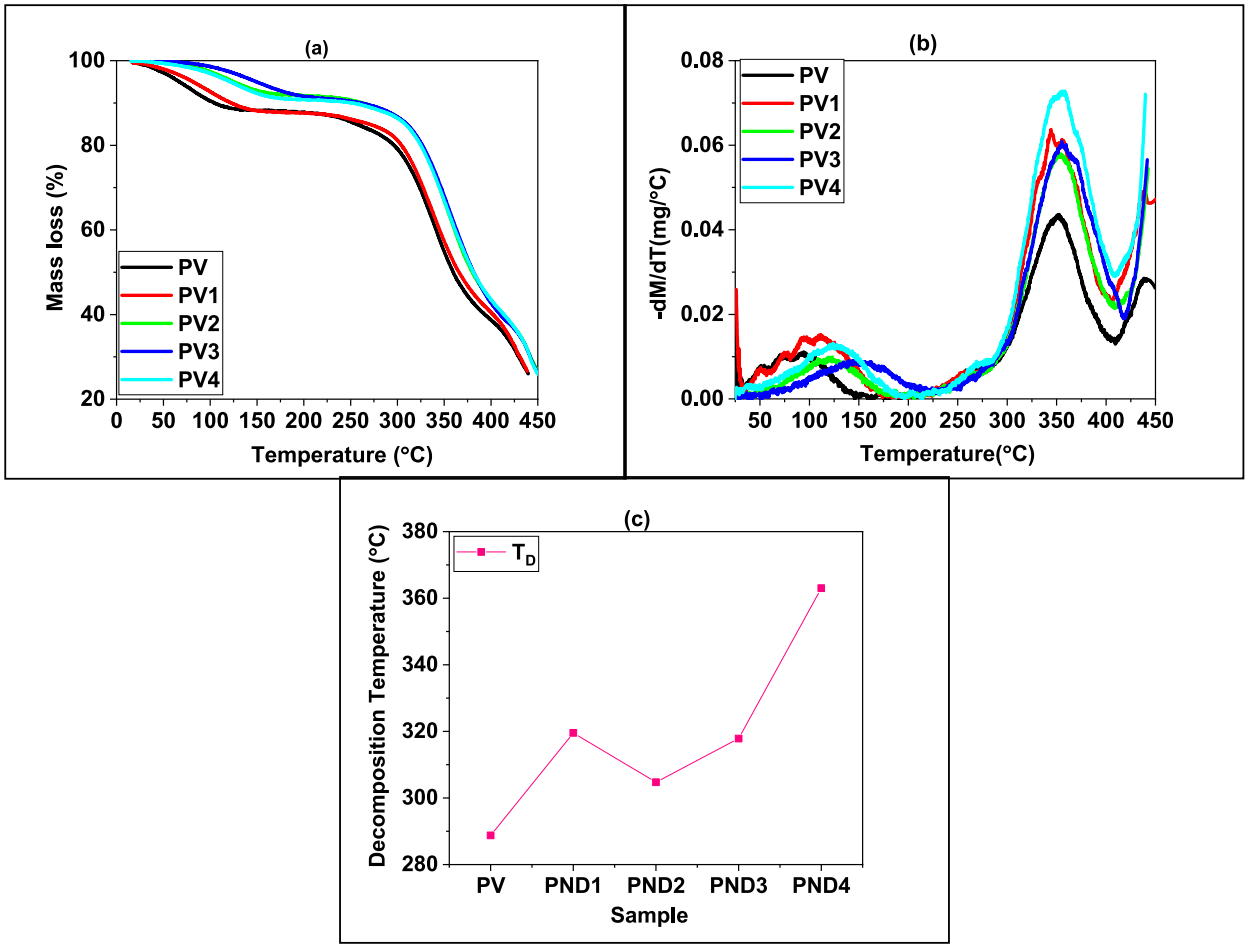

Fig. 3. (a) TGA thermograms, (b) DTG curve and (c) variation of thermal decomposition temperature of PVA- NDs composites.

3.3. DSC analysis

DSC thermograms for PVA-NDs composite are shown in Fig. 4(a). The endotherms assigned the glass transition temperature (Tg) and Tm of pure polymer, PV, around 127 °C and 189 °C, respectively. However, with the increase in NDs content, a significant enhancement in Tg and a slight change in Tm were observed, as reported earlier [57]. NDs disturbed the ordered packing of polymer chains by steric effect and hydrogen bonding. As a result, the short and simple hydroxyl groups became longer, making the crystalline structure rigid and decreasing the crystallinity [55].

Fig. 4(b) presents the variation of Tg with respect to the NDs content. The decrease in Tg at lower NDs concentration (PND1, PND2) might be related to the interaction of NDs with crystalline regions without affecting the amorphous region of PVA [58]. Lower concentrations increased the space between polymer chains. Thus, polymer chains can move freely over one another even at lower temperatures. The improvement in Tg from 127 °C to ~155 °C at higher NDs concentrations (PND3, PND4) might be attributed to higher chain compactness due to the interaction between PVA and NDs, which restricted their thermal actions [55,59]. The degree of crystallinity of PVA composites was calculated using equation (1) [52].

$$\chi_{c=}\frac{\Delta H_m}{w\Delta H_m^0} \tag{1}$$

Where w is the weight fraction of the PVA composite, ΔH_m is the heat of fusion at the melting point, and ΔH_m^0 is the heat of fusion of 100 % crystalline PVA (~139J/g).

A variation in percent crystallinity with the increase in the NDs content is shown in Fig. 4(c). The lowest NDs (PND1) slightly improved (~1 %) the percent crystallinity. The depression of Tm and the broadening of the melting endotherm at higher ND concentrations (PND2, PND3, PND4) indicated the dominance of the amorphous phase [28]. The interaction between the functional groups of NDs with PVA hindered the crystallization process. An increase in hydrogen bonding between PVA and NDs disturbed the regularity of polymer chains [54]. XRD results also support the decrease in polymer crystallinity with NDs content.

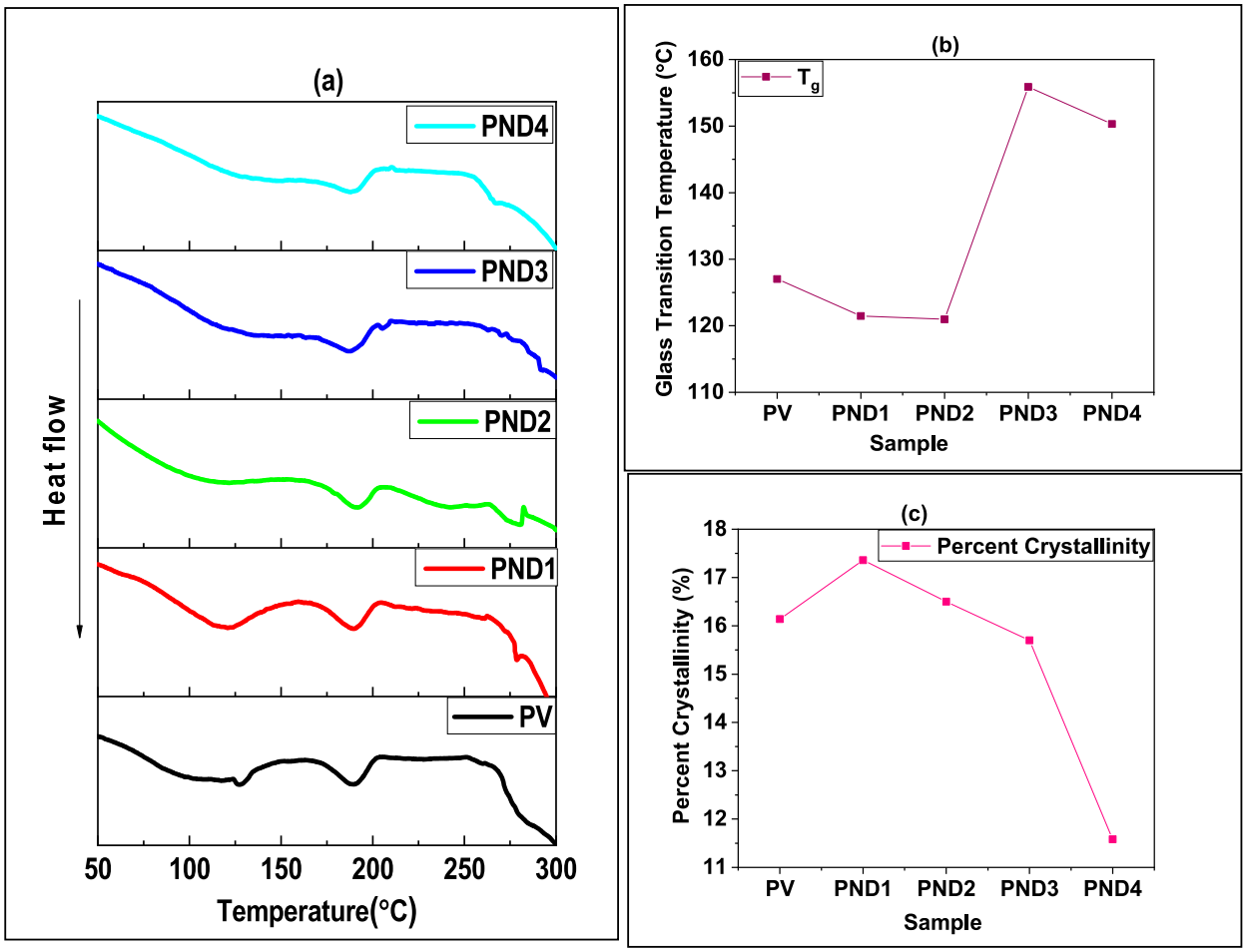

Fig. 4. (a) DSC thermograms, variation of (b) Glass transition temperature and (c) Percent crystallinity of PVA -NDs composites.

The thermal analysis is summarized in Table S2. It is revealed that a small amount of NDs acted as effective degradation-resistant reinforcement in the PVA matrix, leading to the enhanced thermal stability of the composite. The interactions restricted the macromolecule's thermal action while increasing the rigidity of the macromolecular chain and increasing the energy required for movement and breakage of the polymeric chain [55]. The obstruction of decomposition was further confirmed with the enthalpy, indicating more heat absorption in the composite compared to the pristine PVA [58]. The results also indicated that the Tm was far below the Td of PVA. Therefore, the excellent melt processing ability of PVA-NDs makes them a potential candidate for the packaging industry, mainly food packaging [57].

An enhancement in electrical conductivity was also observed due to restricted segmental motions of the polymer chains. The details are mentioned in the supporting information.

3.4. Tensile behaviour of tensile strength of the nanocomposite

The stress-strain curves of the PVA composite at various NDs content are illustrated in Fig. 5(a). The stress-strain curves of the composite exhibited a similar trend to that of PVA but at a different magnitude. Compared to pure PVA, an increment in tensile strength and elongation at break was observed with the addition of NDs in the PVA matrix, especially for PND4. These results are in agreement with Famkar et al. [32]. Significant thermal stability, as suggested by DSC and TGA results, indicated high tensile strength of bonding. Therefore, an increase in melting enthalpy positively affects the mechanical properties of PVA [58].

Fig. 5(b) shows the variation of tensile strength and elongation at break for different NDs content. High mechanical strength suggests that the small size and uniform dispersion of NDs attained a large interfacial area, resulting in a strong interaction between PVA and NDs. The covalent cross-linking with NDs restricts the mobility experienced by the polymer chains in the composite that had an electrostatic attraction with other polymer chains [60]. The application of tensile stress resulted in mechanical interlocking due to the pulling-out phenomenon. Finally, the dissipated energy increased the mechanical strength [18].

An increasing trend in elongation at break with an increase in NDs contents is depicted in Fig. 5(c). The PVA chains experienced lesser flexibility due to the nanoconfinement of the NDs. A large cohesive force is associated with NDs. The applied stress changed the alignment of NDs and relaxed the PVA chains. The enhancement in elongation indicates that NDs are oriented in the direction of applied stress, resulting in efficient interfacial stress transfer [61]. NDs interfaced the hydrogen bonds and van der Waals forces between the PVA chain, making it more flexible. PVA chains elongate without creating cavitation at the interface of the PVA and NDs [62]. Thus, the required key parameters for food packaging, such as large tensile strength and ductility, are obtained at the highest NDs concentration.

3.5. UV visible spectroscopy

Fig. 6(a) illustrates the UV vis absorption spectra of the PVA-NDs composite. The pure PVA films exhibited ~80 % transparency across the visible region. Pure PVA exhibited an absorption peak of ~250 nm. It is related to $\pi \rightarrow \pi^*$ electronic transitions of unsaturated carbonyl bonds of PVA polymer [58]. The increased NDs content decreased the transparency of the composite, which confirms the presence of NDs within the PVA matrix. The NDs filled up the free spaces within the polymeric chains and reduced the light transmission [18,63]. Also, NDs completely blocked UV (200–300 nm) for higher concentrations (PND3 and PND4). The NDs effectively reduce transparency in UVC (0 %), UVB (~85 % above 300 nm), and UVA(~58 %) while maintaining more than 50 % transparency in visible to IR region (400–800 nm). The anti-UV characteristics of NDs can be related to their high refractive index and graphitic shell, which are responsible for the scattering and absorption of UV radiation [34].

Fig. 6(b) shows the variation in the band gap of the PVA composite by varying NDs content. The band gap was calculated using the Tauc relation. A reduction in band gap (5.35–4.05 eV was observed with the enhancement in NDs content. NDs might be responsible

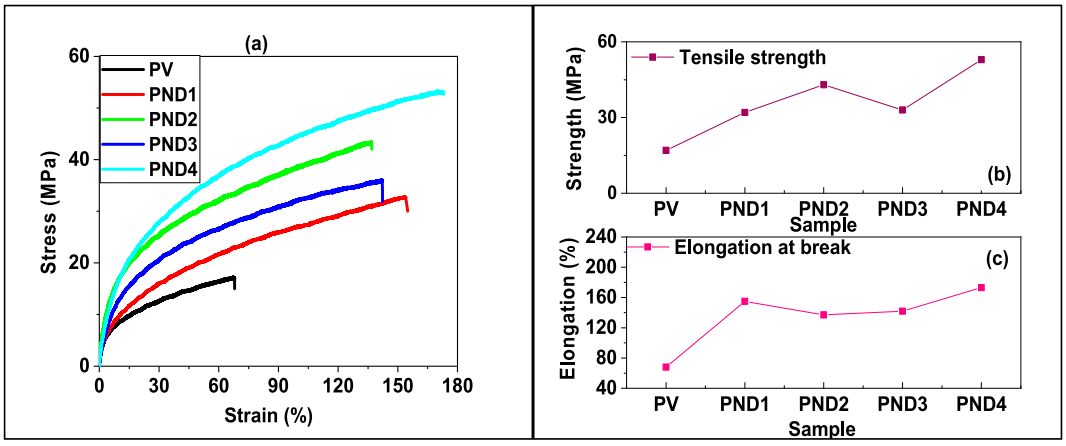

Fig. 5. (a) Stress-Strain curves, variation of (b) tensile strength and (c) elongation at break of PVA-NDs composites.

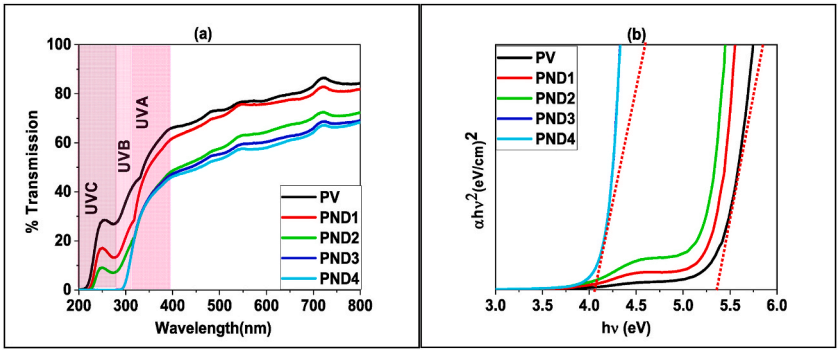

Fig. 6. (a) UV visible spectra and (b) Tauc plot of PVA-NDs composites.

for the creation of defect states between the highest occupied molecular orbital (HOMO) and lowest occupied molecular orbital (LOMO). These localized electronic states formed trapping and recombination centers. Hence, enhancing the low energy transitions resulted in the optical band gap change. The decrease in optical band gap can also reflect an increasing degree of disorder in the films due to changes in the polymer structure. This might be related to local cross-linking within the amorphous phase of the PVA [64,65]. The XRD and DSC results also support these results. These anti-UV characteristics and large transparency must be useful in the food packaging industry.

3.6. FTIR analysis

The FTIR spectra of PVA-NDs nanocomposite are shown in Fig. 7. The intense and broad absorption of ~3000 cm^{-1} corresponded to the CH group of PVA. The band ~2080 cm^{-1} and 1620 cm^{-1} are related to OH group [50]. The bending/deformation CH_2 band and stretching C–C were found around 1429 cm^{-1}, 1384 cm^{-1} and 1268 cm^{-1} [43]. The crystallinity of PVA was ascribed by a 1108 cm^{-1} peak and is associated with the carboxyl stretching band (C–O). However, the peak around 1540 cm^{-1} might be related to the stretching vibration of C═C of the remaining nonhydrolyzed vinyl acetate group of PVA. They might also be related to carboxylate moieties (COO^-) [43,49,53]. The 1090 cm^{-1} might be assigned to the stretching vibration of C–O and the bending vibration of the OH group from an amorphous PVA sequence [49]. Small bands ~400-675 cm^{-1} confirmed the CH vibrations [66]. FTIR spectrum of NDs is shown as Fig. S3 (supporting information). The adsorption of water molecules on NDs surface is confirmed by the dominance of the OH group (3441 cm^{-1}, 2080 cm^{-1},1620 cm^{-1}) in the FTIR spectrum. Table S3 lists the FTIR peaks and their assignments for the pure PVA, NDs and PVA-NDs composite.

Intense alteration in hydrogen bonding between PVA molecules is reflected by modification in the position and shape of the band [53]. The rich surface chemistry of NDs allowed the strong interaction between the surface functional groups of NDs and the polymer matrix. The small shift and band shape or intensity alteration is attributed to the change in the nearest surrounding functional groups [43–45,47,59]. The large surface area of NDs may allow strong interaction of the OH group with the macromolecular chains of PVA, form an interfacial layer on their surface and result in a blue shift (3000–3053 cm^{-1}) with respect to pure PVA [67]. The reduction in the intensity of the OH band after incorporating NDs reveals the improvement of hydrogen bonding of PVA with NDs rather than PVA molecules itself [53]. The broadening of the OH band confirms that the increase in NDs concentration decreases the intermolecular

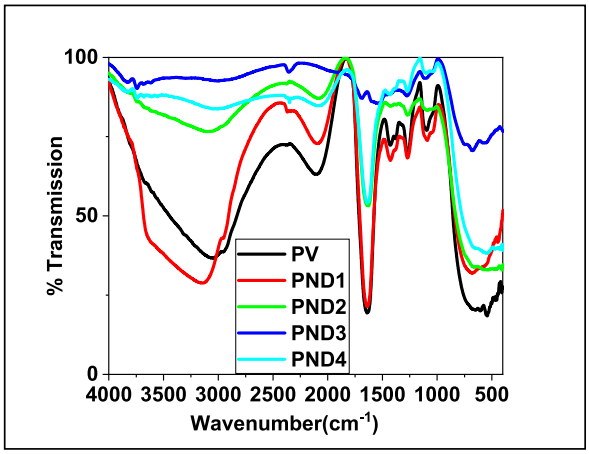

Fig. 7. FTIR spectra of PVA-NDs composites.

interaction between chains and causes expanded space between them [44]. It confirms the interaction of NDs with OH groups of PVA with NDs through hydrogen bonding. Incorporating NDs suppresses the polymeric chain mobility within the host polymer matrix, causing a reduction in relative percent transmittance [68,69]. The C–O stretching vibration peak ~1105 cm^{-1} of the PVA backbone keeps on decreasing with increasing NDs. It supports the previous arguments (XRD and DSC) that NDs in nanocomposite enhance the amorphous zone [19].

3.7. Antibacterial activity of PVA-NDs composite

Fig. 8 (a, b) displays results from the microdilution broth method testing the PVA-NDs composites against *S. aureus* and *E. coli*. The first row is the control (without any antibiotics). Rows second to six show PVA-NDs composite with different ND concentrations. The MIC of the composite was determined by identifying the lowest NDs concentration that showed no antibacterial activity while keeping the PVA concentration fixed.

Fig. 9 shows the effect of NDs content on MIC. The PVA without NDs failed to perform the antibacterial activity. However, PVA-NDs composites were effective for both bacterial strains, *S. aureus* and *E. coli*. A larger amount of NDs expedites the reduction of bacteria as discussed earlier [59]. This might be related to the physicochemical properties (size and presence of functional groups (O–H, C–O)) of NDs. It was assumed that NDs surround the bacterial cells and block essential cellular functions. Functional groups act as efficient catalysts in deforming bacteria cell membrane proteins. As a result, defects are formed in the bacteria cell wall required for good surface contact [41,50]. Beranova et al. [41] utilized low concentrations (5 μg/mL) for partial (~25 %) and large concentrations (~50 μg/mL) of NDs for total growth inhibition. This research work reported fairly a smaller concentration (~16 μg/mL) for total bacterial growth inhibition.

A slightly lower concentration of NDs was enough to sterilize *E. coli* bacteria compared to *S. aureus* (Fig. 9). The higher antibacterial efficacy of NDs against *E. coli* was related to the thinner peptidoglycan layer. The interaction of NDs produced a nanoscale hole in the cell membrane and finally led to the destruction of the cell wall. In the case of *S. aureus, the* thick peptidoglycan layer (~50 % to gram-negative) required more NDs concentration [38].

4. Conclusions

Solution casting methods have fabricated PVA-ND composites. Various diagnostic techniques have investigated the structural, thermal, mechanical, optical and antibacterial properties of composite. In the PVA-NDs composite, NDs restricted the macromolecular motion and decreased the PVA crystallinity. A higher thermal decomposition temperature (~363 °C) compared to melting temperature (~188 °C) confirmed the excellent thermal stability of PVA-NDs. The large surface area of NDs improved the hydrogen bonding of PVA with NDs rather than PVA molecules, enhancing tensile strength (~60 MPa) and ductility (~180 %). The PVA-NDs composite efficiently blocked UVC (100 %), most of the part of UVB (~85 % above 300 nm), and UVA (~58 %). The anti-UV characteristics of NDs can be related to their high refractive index and graphitic shell, which are responsible for the scattering and absorption of UV radiation. The PVA-NDs were effective against *E. coli* and *S. aureus*. However, NDs exhibited more resistance towards *E. coli.* PVA-NDs composite appeared promising for thermally stable, strong, flexible, UV-resistant antibacterial food packaging material.

Data availability

Data will be available on reasonable request to the corresponding author.

Funding

This study is funded by the Universiti Teknologi Malaysia under grant number Q.J130000.2551.21H53 as part of the signal processing research.

CRediT authorship contribution statement

Saman Iqbal: Writing – review & editing, Writing – original draft, Visualization, Methodology, Investigation, Formal analysis, Data curation, Conceptualization. **Muhammad Shahid Rafique:** Supervision, Methodology, Conceptualization. **Nida Iqbal:** Writing – review & editing, Investigation, Formal analysis. **Shazia Bashir:** Resources. **M.B. Malarvili:** Writing – review & editing, Funding acquisition. **Aftab Ahmad Anjum:** Resources.

Declaration of competing interest

The authors declare that they have no known competing financial interests or personal relationships that could have appeared to influence the work reported in this paper.

Appendix A. Supplementary data

Supplementary data to this article can be found online at https://doi.org/10.1016/j.heliyon.2024.e33270.

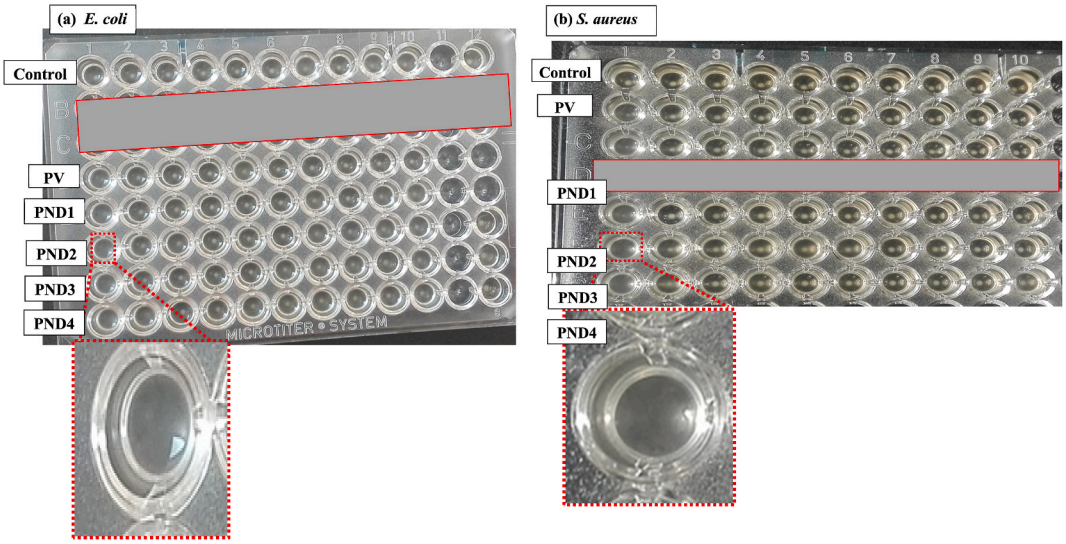

Fig. 8. Antibacterial activity of PVA-NDs composites against (a) *E. coli* and (b) *S. aureus*. The lowest value of MIC is enlarged.

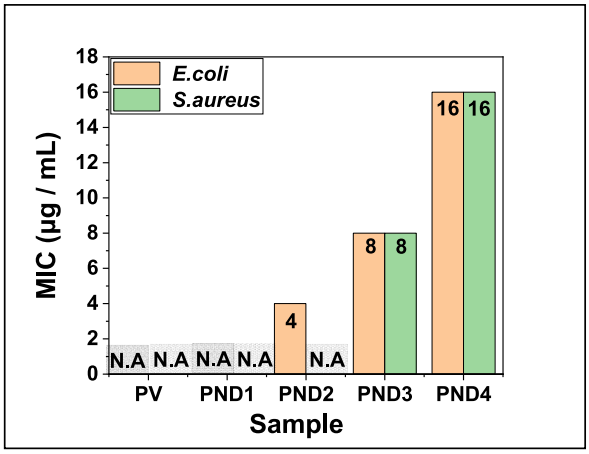

Fig. 9. MIC of PVA- NDs composites against *E. coli* and *S. aureus*.

References

[1] S. Pirsa, F. Mohtarami, Biodegradable film based on barley sprout powder/pectin modified with quercetin and V2O5 nanoparticles: Investigation of physicochemical and structural properties, Heliyon 10 (2024) e25448 (13 pages).
[2] Z. Tabassum, A. Mohan, N. Mamidi, A. Khosla, A. Kumar, P.R. Solanki, T. Malik, M. Girdhar, Recent trends in nanocomposite packaging films utilising waste generated biopolymers: industrial symbiosis and its implication in sustainability, IET Nanobiotechnol. 17 (2023) 127–153.
[3] I. Hamed, A.N. Jakobsen, J. Lerfall, Sustainable edible packaging systems based on active compounds from food processing byproducts: a review, Compr. Rev. Food Sci. Food Saf. 21 (2022) 198–226, https://doi.org/10.1111/1541-4337.12870.
[4] X. Tian, Z. Chen, X. Lu, J. Mu, Q. Ma, X. Li, Soy protein/polyvinyl-alcohol (PVA)-Based packaging films reinforced by nano-TiO2, Polymers 15 (2023), https://doi.org/10.3390/polym15071764.
[5] A.A. Oun, G.H. Shin, J.-W. Rhim, J.T. Kim, Recent advances in polyvinyl alcohol-based composite films and their applications in food packaging, Food Packag. Shelf Life 34 (2022) 100991, https://doi.org/10.1016/j.fpsl.2022.100991.
[6] A.A.B.A. Mohammed, Z. Hasan, A.A. Borhana Omran, A.M. Elfaghi, Y.H. Ali, N.A.A. Akeel, R.A. Ilyas, S.M. Sapuan, Effect of sugar palm fibers on the properties of blended wheat starch/polyvinyl alcohol (PVA) -based biocomposite films, J. Mater. Res. Technol. 24 (2023) 1043–1055, https://doi.org/10.1016/j.jmrt.2023.02.027.
[7] M. Asgher, S.A. Qamar, M. Bilal, H.M.N. Iqbal, Bio-based active food packaging materials: sustainable alternative to conventional petrochemical-based packaging materials, Food Res. Int. 137 (2020) 109625, https://doi.org/10.1016/j.foodres.2020.109625.
[8] A.K. V, M. Hasan, S. Mangaraj, P. M, D.K. Verma, P.P. Srivastav, Trends in edible packaging films and its prospective future in food: a review, Applied Food Research 2 (2022) 100118, https://doi.org/10.1016/j.afres.2022.100118.
[9] N. Qian, X. Gao, X. Lang, H. Deng, T.M. Bratu, Q. Chen, P. Stapleton, B. Yan, W. Min, Rapid single-particle chemical imaging of nanoplastics by SRS microscopy, Proc. Natl. Acad. Sci. USA 121 (2024) e2300582121, https://doi.org/10.1073/pnas.2300582121.
[10] D. Song, L.-W. Ma, B. Pang, R. An, J.-H. Nie, Y.-R. Guo, S. Li, An active bio-based food packaging material of ZnO@plant polyphenols/cellulose/polyvinyl alcohol: DESIGN, characterization and application, Int. J. Mol. Sci. 24 (2023), https://doi.org/10.3390/ijms24021577.

[11] M. Teodorescu, M. Bercea, S. Morariu, Biomaterials of PVA and PVP in medical and pharmaceutical applications: perspectives and challenges, Biotechnol. Adv. 37 (2019) 109–131, https://doi.org/10.1016/J.BIOTECHADV.2018.11.008.

[12] S.Y. Lee, J.T. Kim, K. Chathuranga, J.S. Lee, S.W. Park, W.H. Park, Tannic-acid-enriched poly(vinyl alcohol) nanofibrous membrane as a UV-shie lding and antibacterial face mask filter material, ACS Appl. Mater. Interfaces 15 (2023) 20435–20443, https://doi.org/10.1021/acsami.3c02408.

[13] S. Van Nguyen, B.-K. Lee, PVA/CNC/TiO2 nanocomposite for food-packaging: improved mechanical, UV/water vapor barrier, and antimicrobial properties, Carbohydr. Polym. 298 (2022) 120064, https://doi.org/10.1016/j.carbpol.2022.120064.

[14] B. Liu, J. Zhang, H. Guo, B. Liu, J. Zhang, H. Guo, Membranes Review Research Progress of Polyvinyl Alcohol Water-Resistant Film Materials, 2022, https://doi.org/10.3390/membranes12030347.

[15] Y. Li, X. Xu, H. Zhao, S. Wei, Q. Lu, L. Dai, L. Yang, Dual-bonding structured ternary composite film of poly(vinyl alcohol)–boric acid–nanodiamond, J. Appl. Polym. Sci. 134 (2017) 45449, https://doi.org/10.1002/APP.45449.

[16] D. Rahmadiawan, H. Abral, M.K. Ilham, P. Puspitasari, R.A. Nabawi, S.-C. Shi, E. Sugiarti, A.N. Muslimin, D. Chandra, R.A. Ilyas, R. Zainul, Enhanced UV blocking, tensile and thermal properties of bendable TEMPO-oxidized bacterial cellulose powder-based films immersed in PVA/Uncaria gambir/ZnO solution, J. Mater. Res. Technol. 26 (2023) 5566–5575, https://doi.org/10.1016/j.jmrt.2023.08.267.

[17] Q. Wang, H. Wang, T. Zhang, Z. Hu, L. Xia, L. Li, J. Chen, S. Jiang, Antibacterial activity of polyvinyl alcohol/WO3 films assisted by near-infrared light and its application in freshness monitoring, J. Agric. Food Chem. 69 (2021) 1068–1078, https://doi.org/10.1021/acs.jafc.0c06961.

[18] Y. Li, Y. Chen, Q. Wu, J. Huang, Y. Zhao, Q. Li, S. Wang, Improved hydrophobic, UV barrier and antibacterial properties of multifunctional PVA nanocomposite films reinforced with modified lignin contained cellulose nanofibers, Polymers 14 (2022), https://doi.org/10.3390/polym14091705.

[19] C.M. Yang, K. Chathuranga, J.S. Lee, W.H. Park, Effects of polyphenols on the thermal decomposition, antioxidative, and antimicrobial properties of poly(vinyl alcohol) and poly(vinyl pyrrolidone), Polym. Test. 116 (2022) 107786, https://doi.org/10.1016/j.polymertesting.2022.107786.

[20] S.H. Zaferani, Introduction of polymer-based nanocomposites, in: Polymer-Based Nanocomposites for Energy and Environmental Applications: A Volume in Woodhead Publishing Series in Composites Science and Engineering, 2018, pp. 1–25, https://doi.org/10.1016/B978-0-08-102262-7.00001-5.

[21] A. Kausar, R. Ashraf, M. Siddiq, Polymer/Nanodiamond composites in Li-ion batteries: a review, Polym. Plast. Technol. Eng. 53 (2014) 550–563, https://doi.org/10.1080/03602559.2013.854386.

[22] S. Iqbal, M.S. Rafique, M. Zahid, S. Bashir, M.A. Ahmad, R. Ahmad, Impact of carrier gas flow rate on the synthesis of nanodiamonds via microplasma technique, Mater. Sci. Semicond. Process. 74 (2018) 31–41.

[23] Y.G. Vadym N. Mochalin, Nanodiamond–polymer composites, Diam. Relat. Mater. 58 (2015) 161–171.

[24] O.A. Soboleva, E. v Porodenko, V.G. Sergeev, Oxidized nanodiamond batches as filler for composite films based on polyvinyl alcohol, Russ. J. Gen. Chem. 87 (2017) 1192–1199, https://doi.org/10.1134/S1070363217070234.

[25] M.S.N. Salleh, N.N.M. Nor, N. Mohd, S.F.S. Draman, Water resistance and thermal properties of polyvinyl alcohol-starch fiber blend film, AIP Conf. Proc. 1809 (2017) 020045, https://doi.org/10.1063/1.4975460.

[26] X. Huang, Q. Guo, P. Zhou, C. Lu, G. Yuan, Z. Chen, X. Zhang, Poly(vinyl alcohol)/artificial marble wastes composites with improved melt processability and mechanical properties, Compos. B Eng. 182 (2020) 107628, https://doi.org/10.1016/j.compositesb.2019.107628.

[27] M.M. Amanee D. Salaam, Elijah nyairo and derrick dean, electrospun polyvinyl alcohol/nanodiamond composite scaffolds: morphological, structural, and biological analysis, J Biomater Tissue Eng 4 (2014) 1–8, https://doi.org/10.1166/jbt.2014.1152.

[28] M. Angjellari, E. Tamburri, L. Montaina, M. Natali, D. Passeri, M. Rossi, M.L. Terranova, Beyond the concepts of nanocomposite and 3D printing: PVA and nanodiamonds for layer-by-layer additive manufacturing, Mater. Des. 119 (2017) 12–21.

[29] H. Tian, D. Liu, Y. Yao, S. Ma, X. Zhang, A. Xiang, Effect of sorbitol plasticizer on the structure and properties of melt processed polyvinyl alcohol films, J. Food Sci. 82 (12) (2017) 2926–2932.

[30] P. Posoknistakul, C. Tangkrakul, P. Chaosuanphae, S. Deepentham, W. Techasawong, N. Phonphirunrot, S. Bairak, C. Sakdaronnarong, N. Laosiripojana, Fabrication and characterization of lignin particles and their ultraviolet protection ability in PVA composite film, ACS Omega 5 (2020) 20976–20982, https://doi.org/10.1021/acsomega.0c02443.

[31] Y. Zhang, R. Remadevi, J.P. Hinestroza, X. Wang, M. Naebe, Transparent ultraviolet (UV)-Shielding films made from waste hemp hurd and polyvinyl alcohol (PVA), Polymers 12 (2020), https://doi.org/10.3390/polym12051190.

[32] E. Famkar, G. Pircheraghi, H. Nazockdast, Effectively exerting the reinforcement of polyvinyl alcohol nanocomposite hydrogel via poly(dopamine) functionalized graphene oxide, Compos. Sci. Technol. 217 (2022) 109119, https://doi.org/10.1016/j.compscitech.2021.109119.

[33] H. Chen, R. Li, X. Xu, P. Zhao, S.H.D. Wong, X. Chen, S. Chen, X.-H. Yan, Citrate-based fluorophores in polymeric matrix by easy and green in situ synthesis for full-band UV shielding and emissive transparent display, J. Mater. Sci. 54 (2019), https://doi.org/10.1007/s10853-018-2933-9.

[34] Q. Lin, R.H.J. Xu Xu, N. Yang, A.A. Karim, X.J. Loh, K. Zhang, UV protection and antioxidant activity of nanodiamonds and fullerenes for sunscreen formulations, ACS Appl. Nano Mater. 2 (2019), https://doi.org/10.1021/acsanm.9b01698.

[35] J. Pulit-Prociak, A. Staroń, M. Prokopowicz, K. Magielska, M. Banach, Analysis of antimicrobial properties of PVA-based coatings with silver and zinc oxide nanoparticles, J. Inorg. Organomet. Polym. Mater. 31 (2021) 2306–2318, https://doi.org/10.1007/s10904-020-01838-6.

[36] J. Pulit-Prociak, A. Staroń, P. Staroń, A. Chmielowiec-Korzeniowska, A. Drabik, L. Tymczyna, M. Banach, Preparation and of PVA-based compositions with embedded silver, copper and zinc oxide nanoparticles and assessment of their antibacterial properties, J Nanobiotechnology 18 (2020) 148, https://doi.org/10.1186/s12951-020-00702-6.

[37] W. Hanif, A. Hardiansyah, A. Randy, L.A.T.W. Asri, Physically crosslinked PVA/graphene-based materials/aloe vera hydrogel with antibacterial activity. https://doi.org/10.1039/d1ra04992e, 2021.

[38] W. Cao, X. Peng, X. Chen, X. Wang, J. Feng, Q. Li, H. Chen, C. Jiang, Z. Ye, X. Xing, Facile synthesis of cationic polymer functionalized nanodiamond with high dispersity and antibacterial activity, (n.d.). https://doi.org/10.1007/s10853-016-0475-6.

[39] S. Iqbal, M.S. Rafique, S. Akhtar, N. Iqbal, F. Idrees, A. Mahmood, Role of hydrogen flow rate for the growth of quality nanodiamonds via microplasma technique, Materials Innovations 2 (2022) 214–224, https://doi.org/10.54738/MI.2022.2804.

[40] E. P, M. J, C.Y. C, Y, P. C, C.L. C, A. Chatterjee, Antibacterial effect of ultrafine nanodiamond against gram-negative bacteria Escherichia coli, J. Biomed. Opt. 20 (2015) 051014.

[41] S. Szunerits, A. Barras, R. Boukherroub, Antibacterial applications of nanodiamonds, Int J Environ Res Public Health 13 (2016) 413.

[42] M. Balouiri, M. Sadiki, S.K. Ibnsouda, Methods for in vitro evaluating antimicrobial activity: a review, J Pharm Anal 6 (2016) 71–79, https://doi.org/10.1016/J.JPHA.2015.11.005.

[43] N. Ahad, E. Saion, E. Gharibshahi, Structural, thermal, and electrical properties of PVA-sodium salicylate solid composite polymer electrolyte, J. Nanomater. 2012 (2012) 94.

[44] S. Bhavani, Y. Pavani, M. Ravi, K.K. Kumar, V.V.R.N. Rao, Structural and electrical properties of pure and nicl 2 doped pva polymer electrolytes, Am. J. Polym. Sci. 3 (2013) 56–62.

[45] S. Morimune, M. Kotera, T. Nishino, K. Goto, K. Hata, Poly (vinyl alcohol) nanocomposites with nanodiamond, Macromolecules 44 (2011) 4415–4421.

[46] Y. Zhang, Q. Hua, J.M. Zhang, Y. Zhao, H. Yin, Z. Dai, L. Zheng, J. Tang, Enhanced thermal and mechanical properties by cost-effective carboxylated nanodiamonds in poly (vinyl alcohol), Nanocomposites 4 (2018) 58–67.

[47] C.P. Singh, P.K. Shukla, S.L. Agrawal, Ion transport studies in PVA:NH4CH3COO gel polymer electrolytes, High Perform. Polym. 32 (2020) 208–219, https://doi.org/10.1177/0954008319898242.

[48] S.B. Aziz, R.T. Abdulwahid, M.A. Rasheed, O.Gh Abdullah, H.M. Ahmed, Polymer blending as a novel approach for tuning the SPR peaks of silver nanoparticles, Polymers 9 (2017), https://doi.org/10.3390/polym9100486.

[49] A. Kumar, Nanofibers, INTECH, 2010, p. 438.

[50] S. Iqbal, M.S. Rafique, N. Iqbal, S. Akhtar, A.A. Anjum, M.B. Malarvili, Synergistic effect of Silver-Nanodiamond composite as an efficient antibacterial agent against E. coli and S. aureus, Heliyon 10 (2024) e30500, https://doi.org/10.1016/j.heliyon.2024.e30500.

[51] S. Iqbal, M.S. Rafique, S. Akhtar, N. Liaqat, N. Iqbal, R. Ahmad, A comparative study on finding an effective root for the introduction of hydrogen into microplasma during diamond growth, J. Phys. Chem. Solid. 122 (2018) 72–86.
[52] T. Remis, P. Belsky, T. Kovarik, J. Kadlec, M. Ghafouri Azar, R. Medlín, V. Vavruňková, K. Deshmukh, K.K. Sadasivuni, Study on structure, thermal behavior, and viscoelastic properties of nanodiamond-reinforced poly (vinyl alcohol) nanocomposites, Polymers 13 (2021) 1426.
[53] S.K. Sharma, J. Prakash, P.K. Pujari, Effects of the molecular level dispersion of graphene oxide on the free volume characteristics of poly(vinyl alcohol) and its impact on the thermal and mechanical properties of their nanocomposites, Phys. Chem. Chem. Phys. 17 (2015) 29201–29209, https://doi.org/10.1039/C5CP05278E.
[54] B. Gupta, R. Agarwal, M. Sarwar Alam, Preparation and characterization of polyvinyl alcohol-polyethylene oxide-carboxymethyl cellulose blend membranes, J. Appl. Polym. Sci. 127 (2013) 1301–1308, https://doi.org/10.1002/app.37665.
[55] J. Ahmad, K. Deshmukh, M. Habib, M. Hägg, Influence of TiO nanoparticles on the morphological, thermal and solution properties of PVA/TiO nanocomposite membranes, Arabian J. Sci. Eng. 39 (2014) (Springer Science & Business Media BV).
[56] M.T. Taghizadeh, N. Sabouri, Thermal degradation behavior of polyvinyl alcohol/starch/carboxymethyl cellulose/clay nanocomposites, Universal Journal of Chemistry 1 (2013) 21–29.
[57] T.S. Gaaz, A.B. Sulong, M.N. Akhtar, A.A.H. Kadhum, A.B. Mohamad, A.A. Al-Amiery, Properties and applications of polyvinyl alcohol, halloysite nanotubes and their nanocomposites, Molecules 20 (2015) 22833–22847.
[58] K.K. Dey, P. Kumar, R.R. Yadav, A. Dhar, A.K. Srivastava, CuO nanoellipsoids for superior physicochemical response of biodegradable PVA, RSC Adv. 4 (2014) 10123–10132.
[59] B. Reddy (Ed.), Advances in Nanocomposites - Synthesis, Characterization and Industrial Applications, 2011, p. 980.
[60] R.N. Oliveira, R. Rouzé, B. Quilty, G.G. Alves, G.D.A. Soares, R. Thiré, G.B. McGuinness, Mechanical properties and in vitro characterization of polyvinyl alcohol-nano-silver hydrogel wound dressings, Interface Focus 4 (2014) 20130049.
[61] T.U. Patro, H.D. Wagner, Layer-by-layer assembled PVA/Laponite multilayer free-standing films and their mechanical and thermal properties, Nanotechnology 22 (2011) 455706.
[62] T. Kaur, A. Thirugnanam, K. Pramanik, Tailoring the in vitro characteristics of poly(vinyl alcohol)-nanohydroxyapatite composite scaffolds for bone tissue engineering, J. Polym. Eng. 36 (2016) 771, https://doi.org/10.1515/polyeng-2015-0252.
[63] G. De, J.C. Fernandes, P.H. Campelo, J. de Abreu Figueiredo, H.J. Barbosa De Souza, M.R. Sarkis, P. Joele, M.I. Yoshida, & Lúcia De Fátima, H. Lourenço, Effect of polyvinyl alcohol and carboxymethylcellulose on the technological properties of fish gelatin films, Sci. Rep. | 12 (123AD) 10497. https://doi.org/10.1038/s41598-022-14258-y.
[64] H.K.H.G. Sudha Kamath M. K, R. Chandramani, M.C. Radhakrishna, PVP Influence on PVA crystallinity and optical band gap, Arch. Phys. Res. 6 (2015) 18–21.
[65] E.M. Abdelrazek, A.M. Hezma, A. El-Khodary, A.M. Elzayat, Spectroscopic studies and thermal properties of PCL/PMMA biopolymer blend, Egyptian Journal of Basic and Applied Sciences (2019), https://doi.org/10.1016/j.ejbas.2015.06.001.
[66] L. Pramatarova, D. Mitev, E. Pecheva, E. Radeva, G. Altankov, N. Krasteva, P. Montgomery, R. Dimitrova, R. Sammons, T. Hikov, The Advantages of Polymer Composites with Detonation Nanodiamond Particles for Medical Applications, Citeseer, 2011.
[67] C.-M. Tang, Y.-H. Tian, S.-H. Hsu, Poly (vinyl alcohol) nanocomposites reinforced with bamboo charcoal nanoparticles: mineralization behavior and characterization, Materials 8 (2015) 4895–4911.
[68] A. Afzal, M.S. Rafique, N. Iqbal, A.A. Qaiser, A.W. Anwar, S.S. Iqbal, Synergistic effect of functionalized nanokaolin decorated MWCNTs on the performance of cellulose acetate (CA) membranes spectacular, Nanomaterials 6 (2016) 79, https://doi.org/10.3390/nano6040079.
[69] Y. Shi, D. Xiong, J. Li, K. Wang, N. Wang, In situ repair of graphene defects and enhancement of its reinforcement effect in polyvinyl alcohol hydrogels, RSC Adv. 7 (2017) 1045–1055, https://doi.org/10.1039/C6RA24949C.